RESEARCH PROJECT AT UNIVERSITY OF NEVADA, RENO

QUARTERLY REPORT

September 1, 2018 to November June 30, 2018 Period

Year 2 Project

Shake Table Studies of a Bridge System with ABC Connections

Submitted by

M. Saiidi, A. Itani, M. Moustafa, and E. Shoushtari

Department of Civil and Environmental Engineering

University of Nevada, Reno

Reno, Nevada

Submitted

December 2018

TABLE OF CONTENTS

Year 2 Project: Shake Table Studies of a Bridge System with ABC Connections

UNR Project Website: http://wolfweb.unr.edu/homepage/saiidi/USDOT/index.html
ABC-UTC Project Website: >>> ABC-UTC Webmaster—please update <<<<<<

A. Description of Research Project

ABC connections for prefabricated members are particularly critical in moderate and high seismic zones because earthquake forces place high demand on inelastic deformation of adjoining columns. Structural integrity of the bridge has to be maintained by capacity-protected connections that experience no or little damage.

Various ABC connections have been developed and investigated in the past few years. Because of the critical role of bridge columns, the majority of these connections for column ends at foundation and cap beams. In addition to column connections, superstructure to pier cap connections are also important to ensure that no plastic deformations are developed within the superstructure. Five types of ABC column connections have been developed [Ref. 1-57], each with a variety of details:

1. Grouted Duct (GD) Connections
2. Mechanical Bar Splices
3. Pocket Connections
4. Pipe Pin Connections
5. Rebar Hinge Connections

Superstructure precast concrete or steel girder to pier cap seismic connections are also of different types and details depending on the type of girder (steel or concrete) and the mechanism to provide positive moment capacity at the superstructure cap beam interface.

Except for studies in Ref. 26 and 62, all the other reported studies on ABC connections have been on components consisting of single or a subassembly of part of bridges. Component studies have been essential in understanding the local behavior of connections and have provided invaluable information that is beginning to help formulate seismic design guidelines for ABC connections. However, important questions remain on the total bridge seismic response when these connections are integrated in a bridge system. For example, it is not known how "simple for dead, continuous for live (SDCL)" connections behave under seismic loading when the girders are integrated with precast cap beams and column pocket connections. The studies in Ref. 26 and 62 are on innovative concepts using advanced materials that are still emerging. Those studies do not directly address conventional reinforced concrete or steel materials and details.

There are three reasons for the lack of data on the seismic response of conventional ABC bridge systems: (1) It has been essential to develop an understanding of ABC connection behavior at the component level before system studies can be undertaken, (2) seismic studies of bridge systems requires unique distributed shake table systems with sufficient capacity to test large-scale bridge models, and (3) bridge system tests are costly because of the number of components involved and the associated labor and laboratory fee costs. The second barrier is addressed by the state-of-the-art shake table testing facility at UNR. The issue of cost can be addressed through allocating a portion of the ABC-UTC funds.

The purpose of the study proposed at UNR using the ABC-UTC funds is to integrate various ABC column and superstructure connections in shake table studies of a large-scale bridge model.

A.2 Contribution to Expanding Use of ABC in Practice

Because satisfactory seismic performance of bridges cannot be guaranteed unless the connections are sound and reliable, states in moderate and high seismic zones have viewed substantial research data on ABC connections as an essential prerequisite before ABC can be embraced. Plausible earthquake-resistant precast component connections have been developed and preliminary design guidelines are emerging. However, a holistic study of ABC bridge system and the effect of interaction and load distribution among bridge components is necessary before bridges with ABC connections can be confidently recommended for adoption in routine bridge design and construction in states that are susceptible to earthquakes. Incorporation of steel girders in this study will generate information and could help expand the options available to bridge designers in moderate and strong seismic zones.

A.3 Research Approach and Methods

The overall objective of the proposed study is to investigate the seismic performance of a large-scale two-span bridge system that integrates some of the more promising ABC connections that have been proof tested. The selection of the connections will be based on the latest state-of-the-art review, a recently developed evaluation document [63], feedback from other ABC-UTC researches, the ABC-UTC-Seismic steering committee, and the AASHTO T-3 committee. A two-span bridge model with concrete substructure, steel girders, and precast deck panels is envisioned. The bridge model will be supported on three shake tables at UNR and will be subjected to bidirectional horizontal seismic loading. Representative earthquake records will be simulated at the pier base and the abutments. The model will be tested under seismic loading of increasing amplitude until failure. Different limit states including the ultimate condition will be investigated. Specific objectives of the project are to determine:

a) Any constructability issues related to assembling various bridge components and connections,
b) interaction among different bridge components,
c) effect of combined gravity and bidirectional seismic loading on ABC connections, the effectiveness of CFRP tendons in minimizing residual displacements under strong earthquakes, and
d) adequacy of emerging seismic design guidelines for ABC connections.

A.4 Description of Tasks to Be Completed in Research Project

The proposed research will consist of the following tasks to accomplish the objectives of the study:

Task 1 – Literature Review **100% Completed**

An in-depth literature search is conducted to identify the most recent test data and analytical results on cyclic load or dynamic load studies of prefabricated bridge elements and their connections. The search includes any tests or analyses of ABC bridge systems subjected to seismic loading. Included is precast deck panels and their connections to girders and to other panels.

Under Task 1 of the study, the literature search is updated and expanded to identify any new information that could potentially enhance the menu of different earthquake-resistant ABC elements and connections.

Task 2 – Evaluate ABC connections and details **100% completed**

The catalog of prefabricated elements and ABC connections is prepared and a rating system is developed to help identify optimum ABC details that factor in seismic performance, ease of construction, time saving, cost, durability, damage susceptibility, etc. For example, prefabricated columns may be solid, segmental, hollow, SCC (self-consolidating concrete) filled hollow columns, concrete-filled steel tubes, concrete-filled FRP (fiber-reinforced polymer) tubes, etc. The relative merit of these alternatives is evaluated. Another example is connection between columns and cap beams. Grouted ducts and pocket connections are among some of the most investigated connections. Another alternative adopted by some states involve the use of mechanical splices. These and any other emerging alternatives are assessed and pros and cons of each are identified. A few alternative SDCL connections under seismic loading have been developed. Relative merit of these connections is evaluated. Past research on SDCL connections for steel girders under seismic loading are limited but current research at the Florida International University could yield practical alternative connections. These details are assessed in collaboration with FIU researchers because one of the main objectives of this research is to study the seismic performance of SDCL connection detail at FIU Phase I of the FIU work aimed at developing a detail that is suited for

seismic application. Phase II of the FIU study includes a component testing of the seismic SDCL detail, before incorporating the connection in the shake table test model. UNR and FIU researcher will maintain close cooperation during the project.

Task 3 – Develop preliminary design for a two-span large-scale bridge model for shake table testing: 100% Completed

Select ABC connection details and prefabricated elements that are ranked at the top of different alternatives are integrated in a, 0.35-scale, straight, two-span bridge models to be tested on the UNR shake tables. The preliminary dimensions of the assumed prototype are shown in Fig. 37. The width and the number of the girders of the bridge are approximately 80% of a bridge for a two-lane highway bridge. The width was reduced to allow for a larger scale of the bridge model. The details in Fig. 37 are preliminary and conceptual at this stage. Preliminary design of the steel girders, the columns, the cap beam, and the deck has begun. All the components will be precast elements except for the portion of the girder to cap beam connection detail that will utilize FIU's SDCL connection detail that requires closure pours. The key details to be decided are column connection to the footing, column-pier cap connection, girder-cap beam connection, deck-girder connection, and connections between adjacent decks. The preliminary shake table test setup is shown in Fig. 38.

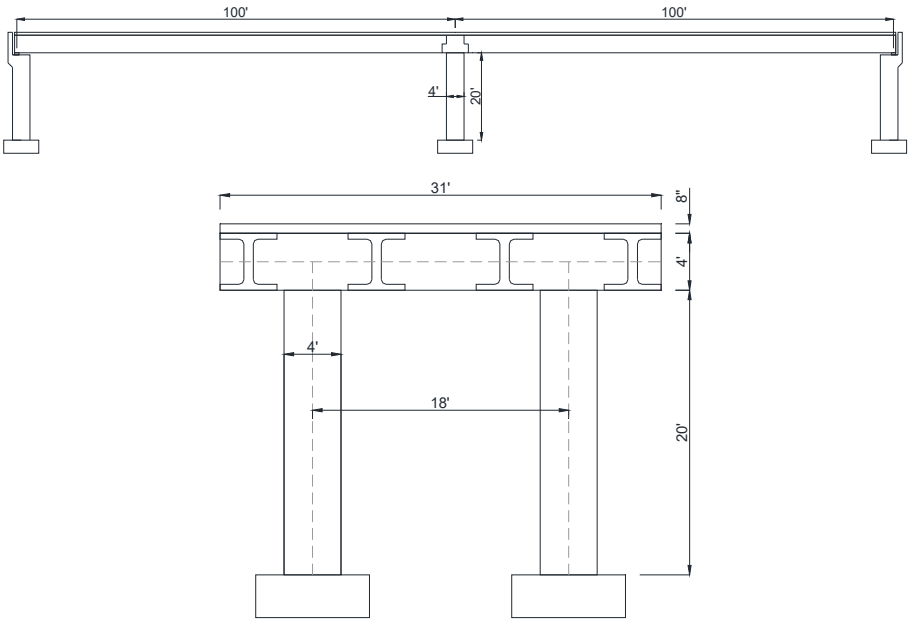

Fig. 37 – Preliminary configuration of the prototype

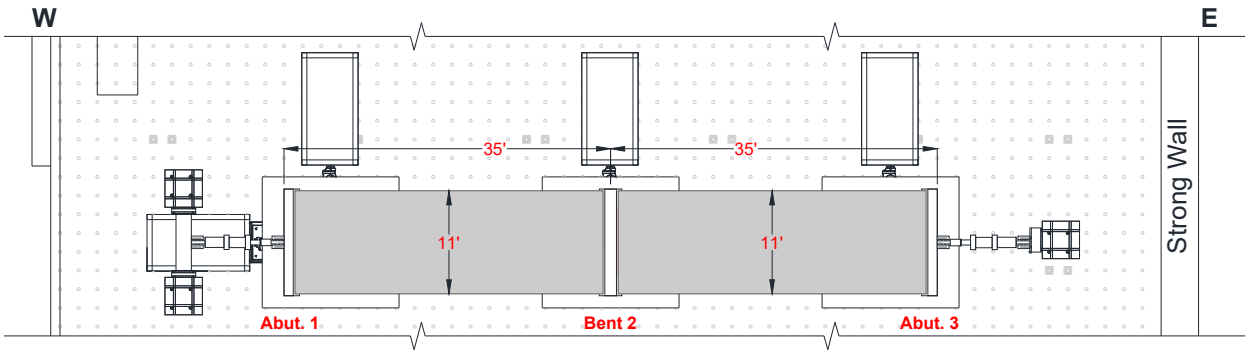

Fig. 38 – Plan view of the preliminary test setup

The preliminary design of the steel superstructure utilizing four steel girders was carried out. Figure 39 shows the details of the steel girders. The girders include welded studs for connection of precast deck panels that are being designed. The cross frame location are marked in the figure. Details of the cross frames are shown in Figure 40. A request was made to the National Steel Bridge Alliance in July for donation of the steel components for the superstructure. Based on discussion between the Director of ABC-UTC and NSBA, the girders, cross frames, and other accessories are to be donated to UNR.

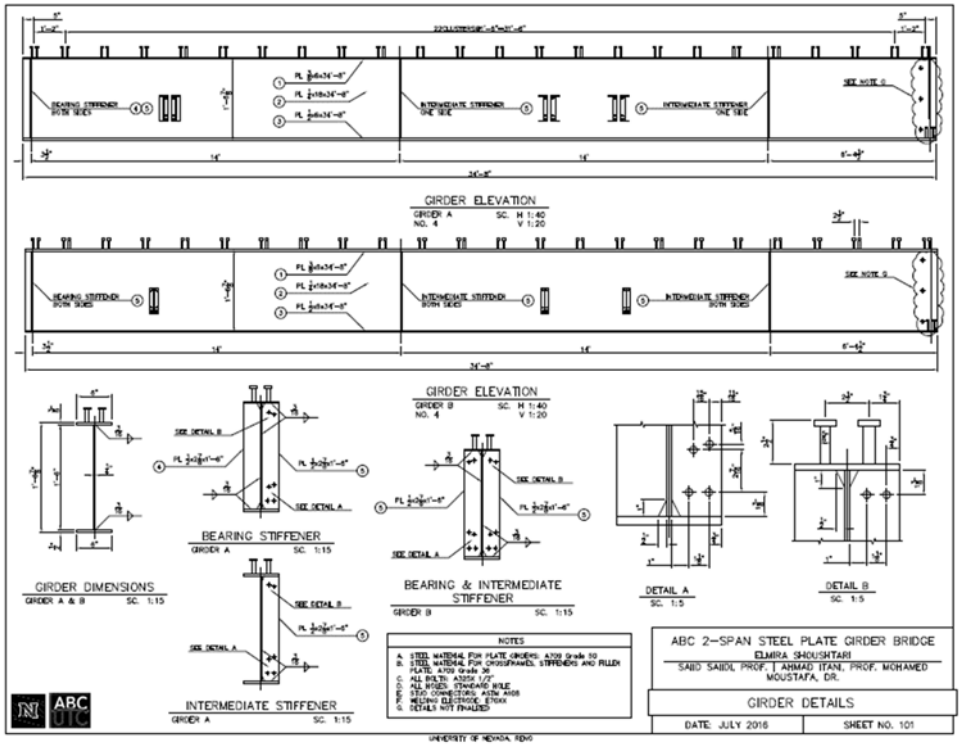

Fig. 39 – Details of superstructure steel plate girders.

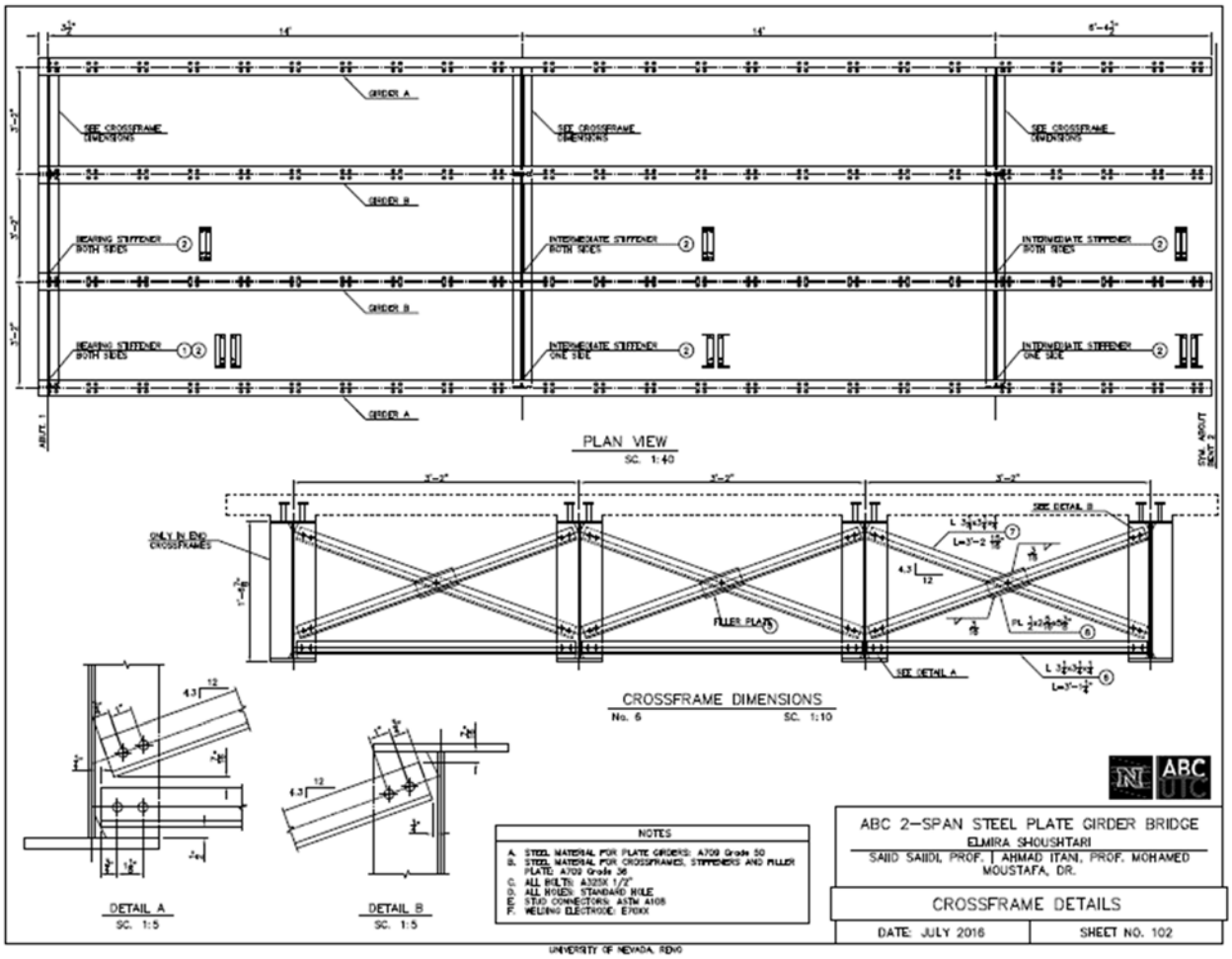

Fig. 40 – Details of superstructure cross frames

Task 4 – Finalize bridge model details, construct and instrument the bridge model, and conduct shake table tests **100% Completed**

The design of the bridge model was completed, and the testing configuration was finalized. The abutment actuators shown in Fig. 38 were eliminated because further detailed nonlinear analysis revealed that they are not necessary for failure testing of the bridge model. With assistance from FIU, a request was submitted to the National Steel Bridge Alliance (NSBA) to donate the steel girders and other superstructure steel components. NSBA has agreed to provide the material to the Reno Iron Work (RIW) for fabrication. NSBA has partially covered the cost of fabrication. The remainder of the fabrication costs are born by the UNR-ABC-UTC budget and donation by RIW. Construction of the two-column bent began. Figures 41-44 show reinforcement or formwork for different components of the pier model. Strain gage layout was finalized and the gages were ordered and received. They have been installed on select rebars in critical parts of the components.

Fig. 41 – Formwork for the precast portion of cap beam

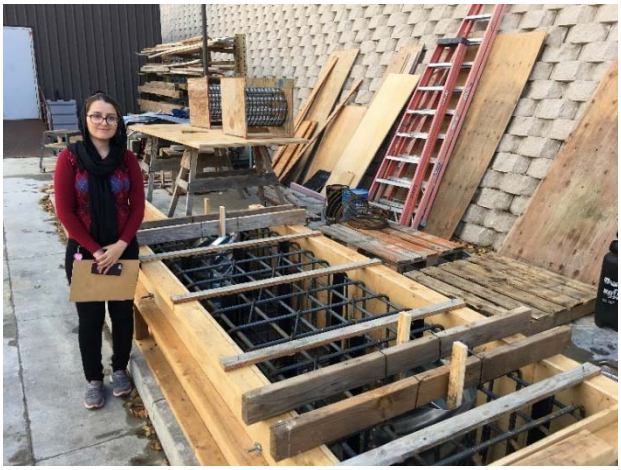

Fig. 42 – Footing reinforcement

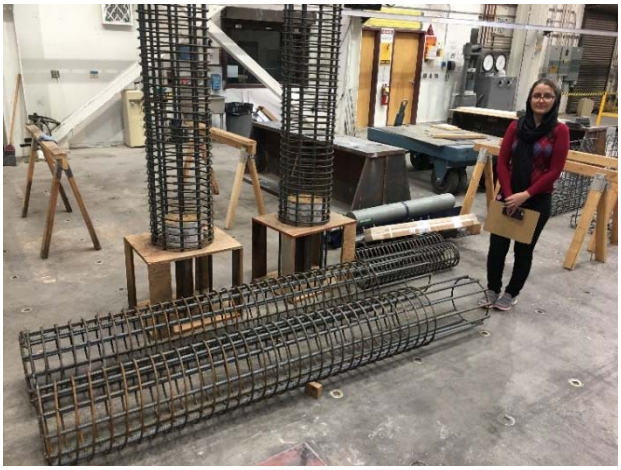

Fig. 43 – Column reinforcement cages

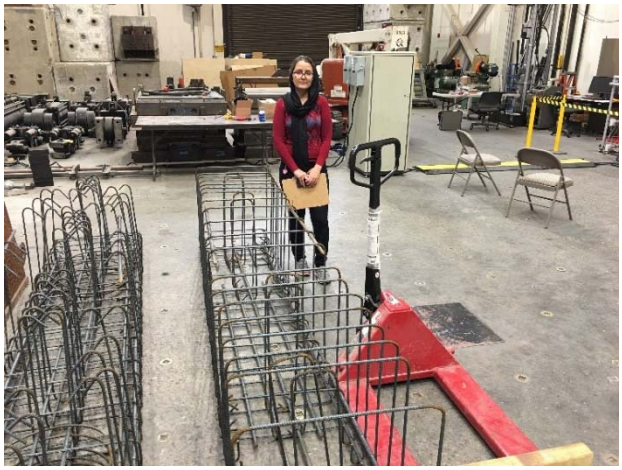

Fig. 44 – Cap beam reinforcement cage

Figure 45 shows the completed footing for the pier. The sockets left in the footing are for column-footing connections. The completed precast columns are shown in Fig. 46. The reduced end bars are two-way hinges that will be inserted into the footing sockets and grouted. The bars at the other end of the columns will be inserted into the grouted ducts in the lower part of the cap beam and extended into the cast-in-place part of the upper part of the cap beam. Figure 47 shows the completed lower part of the cap beam. The holes in the beam indicate the grouted ducts, and the reinforcement extending out of the cap beam are the bars to help complete the remainder of the cap beam.

Fig. 45 – Precast footing with sockets (pockets).

Fig. 46 – Completed precast columns for the bent

Fig. 47 – Completed lower cap beam with corrugated ducts

The design of the deck panel was finalized and a construction bid was obtained. The layout of the deck panels in the vicinity of the pier is shown in Fig. 48. Another activity of the project is securing donation of steel from the National Steel Bridge Alliance, identification of a local steel fabricator, and fabrication of the steel girders and the diaphragm. Figure 39 shows the details of the steel elements of the superstructure.

The construction of the precast deck panels was completed during this period. Figure 49 shows an over view of the deck panel reinforcement and Fig. 50 shows the completed deck panels for one of the spans. The steel reinforcement in the end deck panels in each span extend out to be connected to the SDCL connection at cap beam. Figure 51 shows the extended bars.

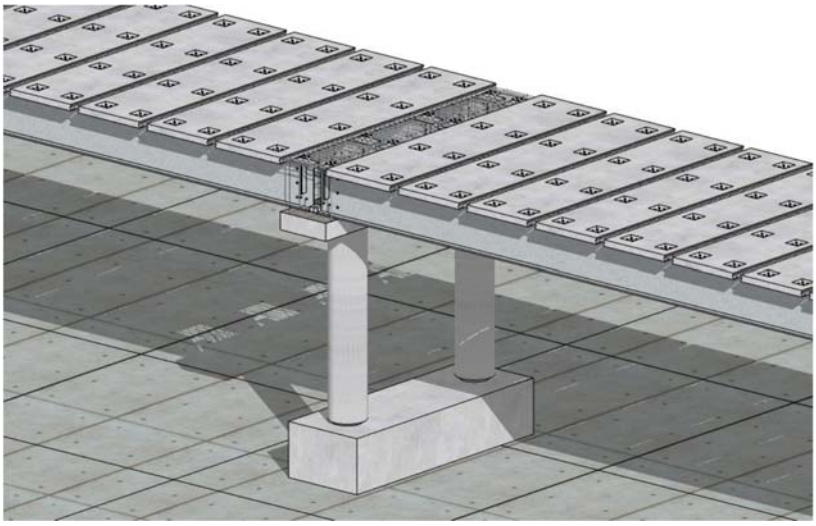

Fig. 48 – Deck panel layout

Fig. 49 – Deck panel steel reinforcement

Fig. 50 – Completed deck panels for one of the spans

Fig. 51 – Edge deck panel with extended reinforcement on the right

The steel plate girders were fabricated. Figure 52 shows the welding of the flanges and the web. Attaching the studs to be inserted in the precast deck panel pockets is shown in Fig. 53. The girder end details were also completed. Figure 54 shows the ends that are to be connected to the SDCL connection at the pier. The holes in the web allow for passage of transverse reinforcement. The steel girders were delivered during this period. The cross braces were attached as shown in Fig. 55.

Fig. 52 – Welding of the flanges to the web

Fig. 53 – Attachment of studs

Fig. 54 – Girder end details for SDCL connection at cap beam

Fig. 55 – Assembled girders with cross braces

The deck panels were placed on the girders and the pockets with studs that had been welded to the girder flanges were filled with a high strength grout. Figure 56 and 57 show the completed grout pockets.

Fig. 56 – End view of superstructure after placing and grouting of pockets

Fig. 57 – Grouted deck pockets

The next step was placing UHPC in the deck joints before the spans were completed and moved to the lab. This was done in early 2018 (Fig. 58), and a minimum of two weeks curing time was allowed before span moves. Moving one of the completed spans is shown in Fig. 59.

Fig. 58 – UHPC in deck joints

Fig. 59 – Moving complete span to lab

The elements of the two-column bent were assembled and secured to the shake table also in early 2018 after sufficient curing of the grouts in the bent connections. Figure 60 shows the view of the pier on the table. Note the column bars and bars in the upper part of the cap beam.

Fig. 60 – Two-column bent secured to the shake table

In approximately one month after assembling the pier, the spans were placed on the abutments and temporary supports adjacent to the pier. Figure 61 shows one of the spans.

Fig. 61 – The east span supported on east abutment and near the pier.

The other span was supported in a similar fashion as shown in Fig. 61. Bearing pads were placed and secured on the lower cap beam, and the spans were gradually lowered to balance the load on both sides of the pier. The upper part of the cap beam was constructed subsequently by placing concrete in the closure pour connecting the girders and the cap beam. UHPC was placed in the upper 2.75 in. to match the thickness of the deck and provide sufficient anchorage for the deck bars that were lapped over the cap beam. The completed bridge model prior to placing all the superimposed mass blocks is shown in Fig. 62.

Fig. 62 – Completed bridge model

The bridge model was instrumented with approximately 300 channels of data the summary of which is listed in Table 1. Not shown are the data channels that are internal to the shake tables.

Table 1 Instrumentation

Type of Instrument	Quantity	# of channels	Type of Instrument	Quantity	# of channels
String pot	22	22	Strain gauge	150	150
Accelerometer	6	18	Rosette	4	12
Novotechnik	64	64	Cameras (GoPro+Video)	20+2	22

Details of the instrumentation are presented on pages 32-39 at the following link: https://wolfweb.unr.edu/homepage/saiidi/ABC/PDFs/TestHandout4-20-18.pdf. The bridge model was subjected to the loading protocol described below.

The bridge was designed for Los Angeles area, Lake Wood, with the latitude and longitude of 33.84926 N, and 118.09252 W, respectively. A site class D was assumed to obtain the AASHTO acceleration design spectrum. Two components of the 1994 Northridge earthquake acceleration history recorded at the Sylmar station, RSN1084_SCS052 (herein called Sylmar052), and RSN1084 _SCS142 (herein called Sylmar142), will be simulated in the shake table test. The former will be applied in the transverse direction, and the latter in the longitudinal direction. To account for the similitude requirements, the time axis of the acceleration record was compressed by a factor of 0.592. This value corresponds to the square root of the dimensional scale length factor.

The amplitude of the design earthquake (DE) was determined so that the peak resultant displacements obtained from the nonlinear dynamic analysis and that obtained from the orthogonal combination of the design displacement demands were approximately the same. As a result, the acceleration records for each component were further scaled by a factor of 0.6. The acceleration, velocity, and displacements histories of the horizontal components for the time scaled design earthquake are shown in Fig. 63. Figure 64 shows the time scaled response spectra of two components and their SRSS resultant as well as scaled AASHTO design spectrum.

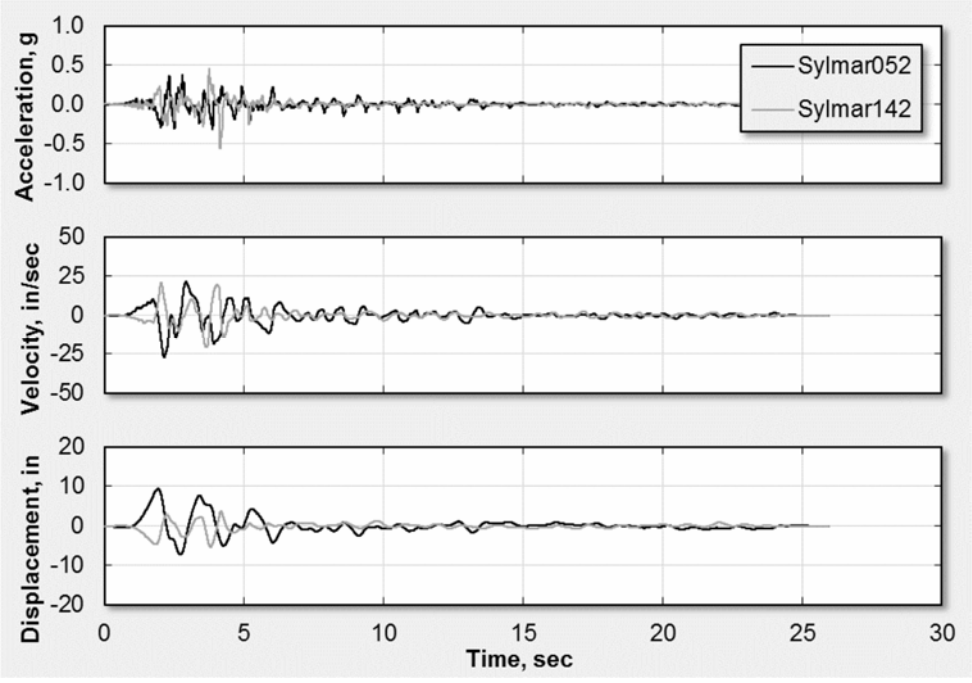

Fig. 63 – Acceleration, velocity, and displacement history of the time scaled design earthquake components

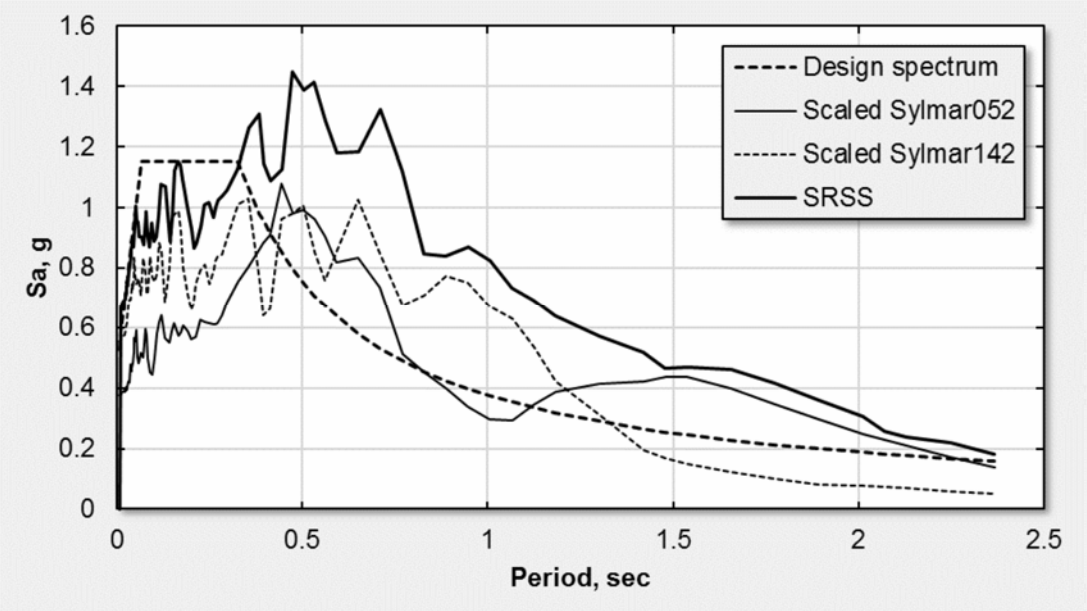

Fig. 64 – Design response spectrum and scaled response spectrum of the ground motion components and their SRSS resultant

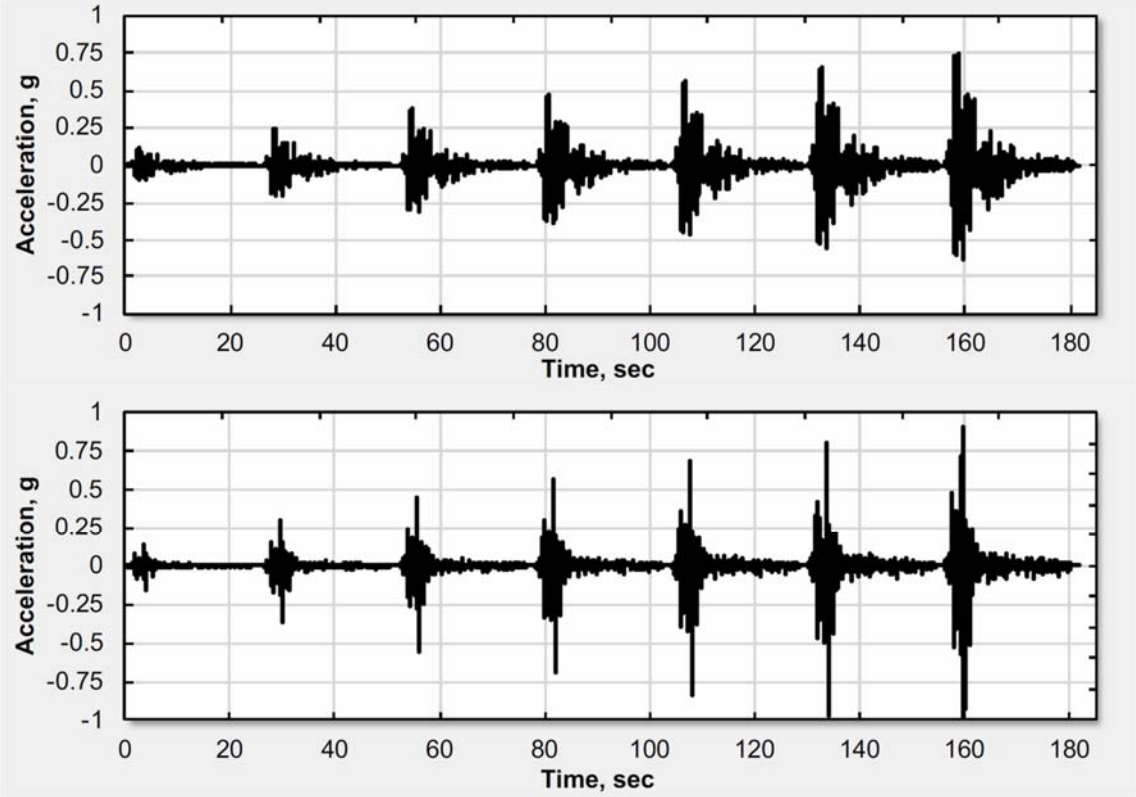

Fig. 65 – Spliced ground motion acceleration history Sylmar 052 (top), and Sylmar142 (bottom)

The loading protocol was determined such that the maximum displacement in each run helps construct the pushover curve from pre-yield status to failure based on the envelope of the hysteresis curve in each direction. The loading protocol starts with 0.3×Sylmar to capture the elastic response

and followed by 0.65×Sylmar and 1.0×Sylmar, continued to 2.0 Sylmar with 0.25×Sylmar increments to capture different damage states. The spliced ground motion acceleration history is shown on Fig. 65. The load factors to be multiplied by the acceleration points to produce the desired amplitude are presented in Table 2. Before applying each run of ground motion, the bridge was subjected to random white noises in the longitudinal and transverse direction to determine the natural frequency and damping ratio. Modal analysis of the bridge model assuming cracked columns showed that the first three modes were in-plane rotation, longitudinal, and transverse with periods of 3.5, 0.67, and 0.59 s, respectively.

Table 2- Shake table loading protocol

Run #	Test type	Scale Factor	PGA (g, longitudinal)	PGA (g, transverse)	%DE
WN1L	White Noise				
WN1T	White Noise				
1		0.18	0.167	0.112	30%
WN2L	White Noise				
WN2T	White Noise				
2		0.39	0.361	0.243	65%
WN3L	White Noise				
WN3T	White Noise				
3		0.60	0.556	0.374	100%
WN4L	White Noise				
WN4T	White Noise				
4		0.75	0.695	0.468	125%
WN5L	White Noise				
WN5T	White Noise				
5		0.90	0.833	0.562	150%
WN6L	White Noise				
WN6T	White Noise				
6		1.05	0.972	0.655	175%
WN7L	White Noise				
WN7T	White Noise				
7		1.20	1.111	0.749	200%
WN8L	White Noise				
WNT	White Noise				

The shake table tests were successfully conducted in April 2018. An additional earthquake run with 225% of design amplitude was applied to the bridge after it was realized that the bridge could still withstand stronger motions than Run 7 (200% design earthquake) shown in Table 2. Select

photos of the observed damage are shown below. As it can be seen all the capacity-protected members and connections remained damage free. However, the columns underwent substantial yielding and damage to concrete at both at the top plastic hinges and the two-way hinges at the base (Figures 66 and 67).

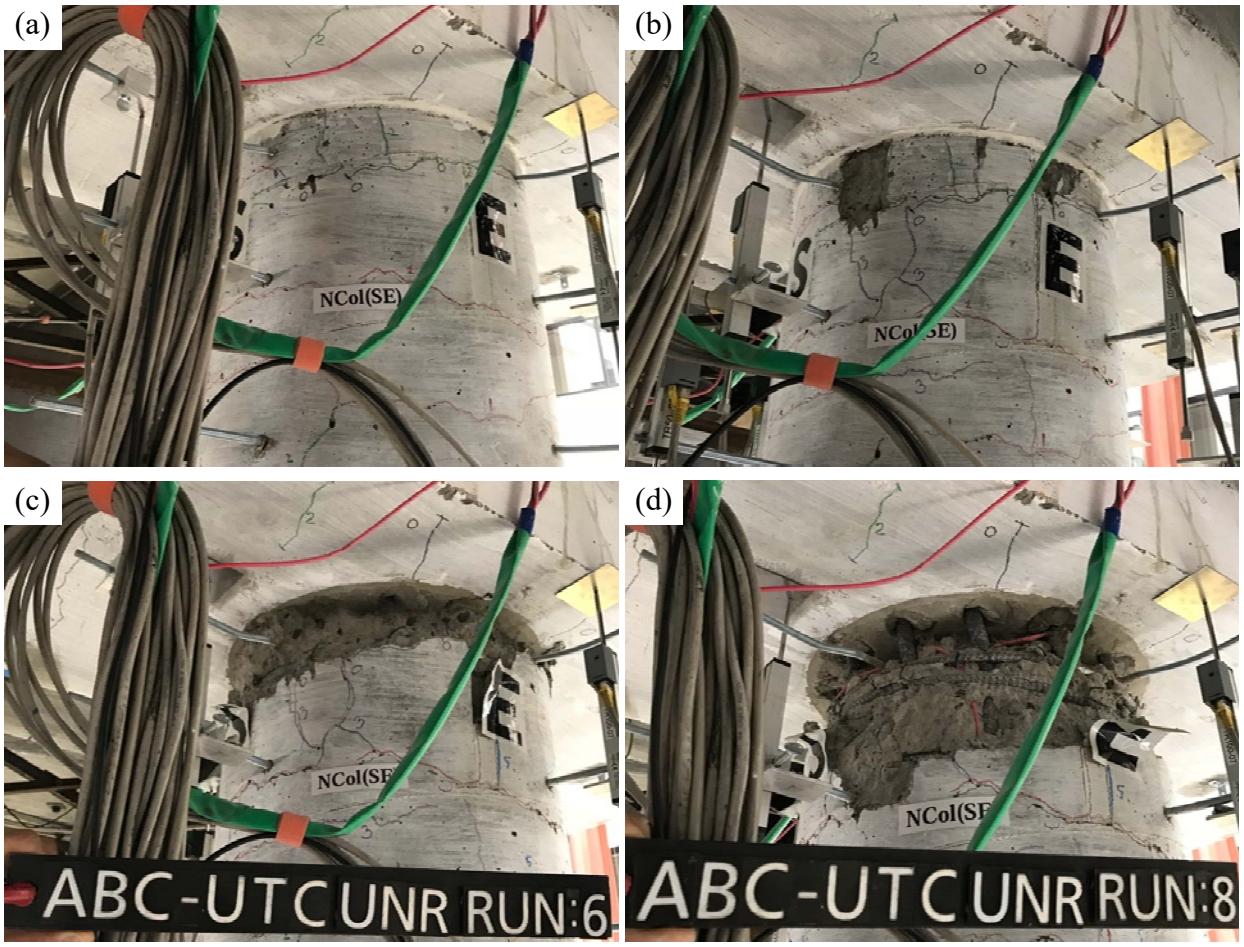

Fig. 66 – Damage progression in the north column, southeast side: (a) Run 2, (b) Run 4, (c) Run 6, (d) Run 8 (Images by Elmira Shoushtari)

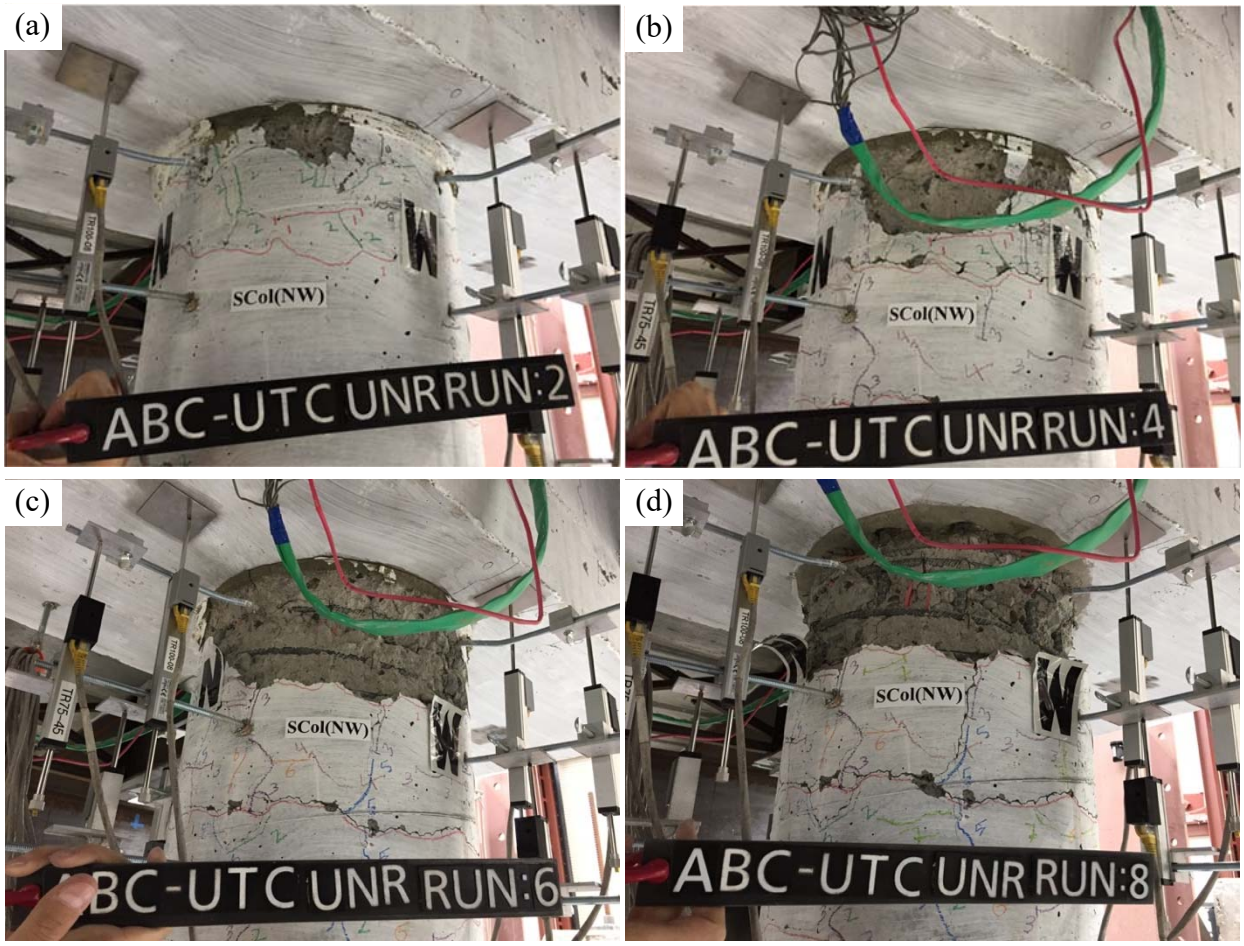

Fig. 67 – Damage progression in the south column, northwest side: (a) Run 2, (b) Run 4, (c) Run 6, (d) Run 8 (Images by Elmira Shoushtari)

There was no damage in the column at the base hinge (Fig. 68). However, there was substantial yielding of the longitudinal steel and spalling of concrete at the hinge throat starting with Run 4. The cap beam to superstructure connections as well as all the deck connections also remained damage free (Fig. 69 and 70).

Fig. 69 – Cap beam to girder connection damage state (Images by Elmira Shoushtari)

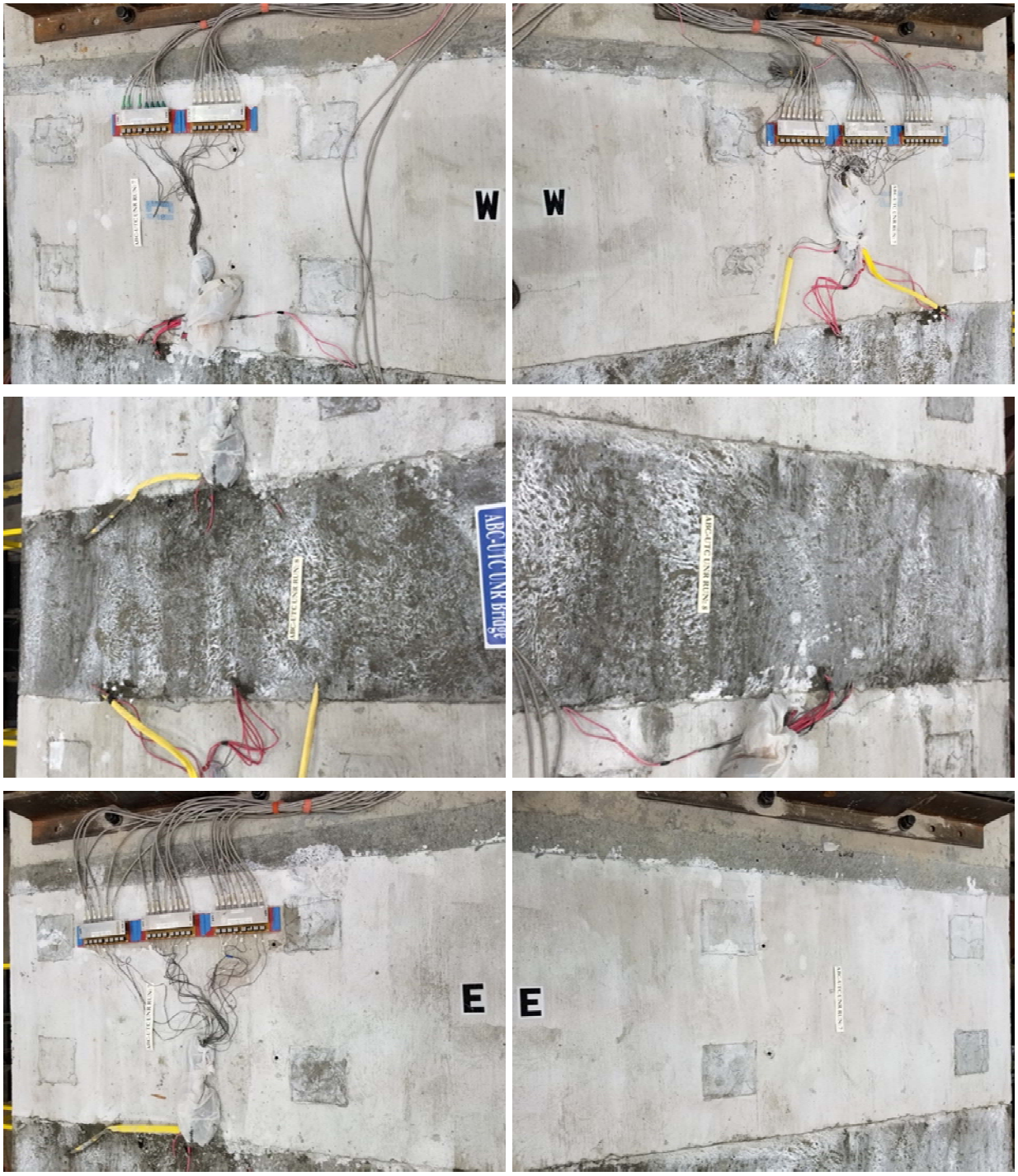

Fig. 70 – Damage states of the superstructure joints (Images by Elmira Shoushtari)

Task 5 – Process and interpret shake table test data and assess seismic performance of bridge model (80% Complete)

Tremendous effort was carried out in processing, scrutinizing, and evaluating the data from the nearly 300 channels of data collected over 8 earthquake runs. Evaluation of the data from all the channels have been completed and processing and plotting of data has begun. A sample of the processed data is presented in the following sections.

The measured force-displacement hysteresis relationships in the longitudinal and transverse direction of the bridge are shown in Fig. 71 and 72, respectively. The data were filtered to eliminate high-frequency responses that do not represent the frequency range of the bridge model. The data for run 1 shows that the model was essentially elastic. Limited nonlinearity mostly due to yielding of the longitudinal bars in the column base hinges and the column top plastic hinges began during run 2. The yielding in run 3 (the design run) was significant, but it was not until run 5 when extent of yielding became substantial. This observation is true for both the longitudinal and transverse responses, but was more prominent in the longitudinal direction of the bridge.

The cumulative force displacement responses for all the eight earthquake runs are shown in Fig. 73 and 74 for the longitudinal and transverse directions, respectively. It is evident that the curves are wide indicating substantial energy dissipation mostly due to plastic hinging of the column ends. The hysteresis loops were stable with little strength degradation even under higher amplitudes. The curves in the longitudinal direction are relatively smooth as they are affected by the combined inelastic action of the columns in that direction. However, the uneven nonlinearity of the columns affected the shape of the curves in the transverse direction making them less smooth.

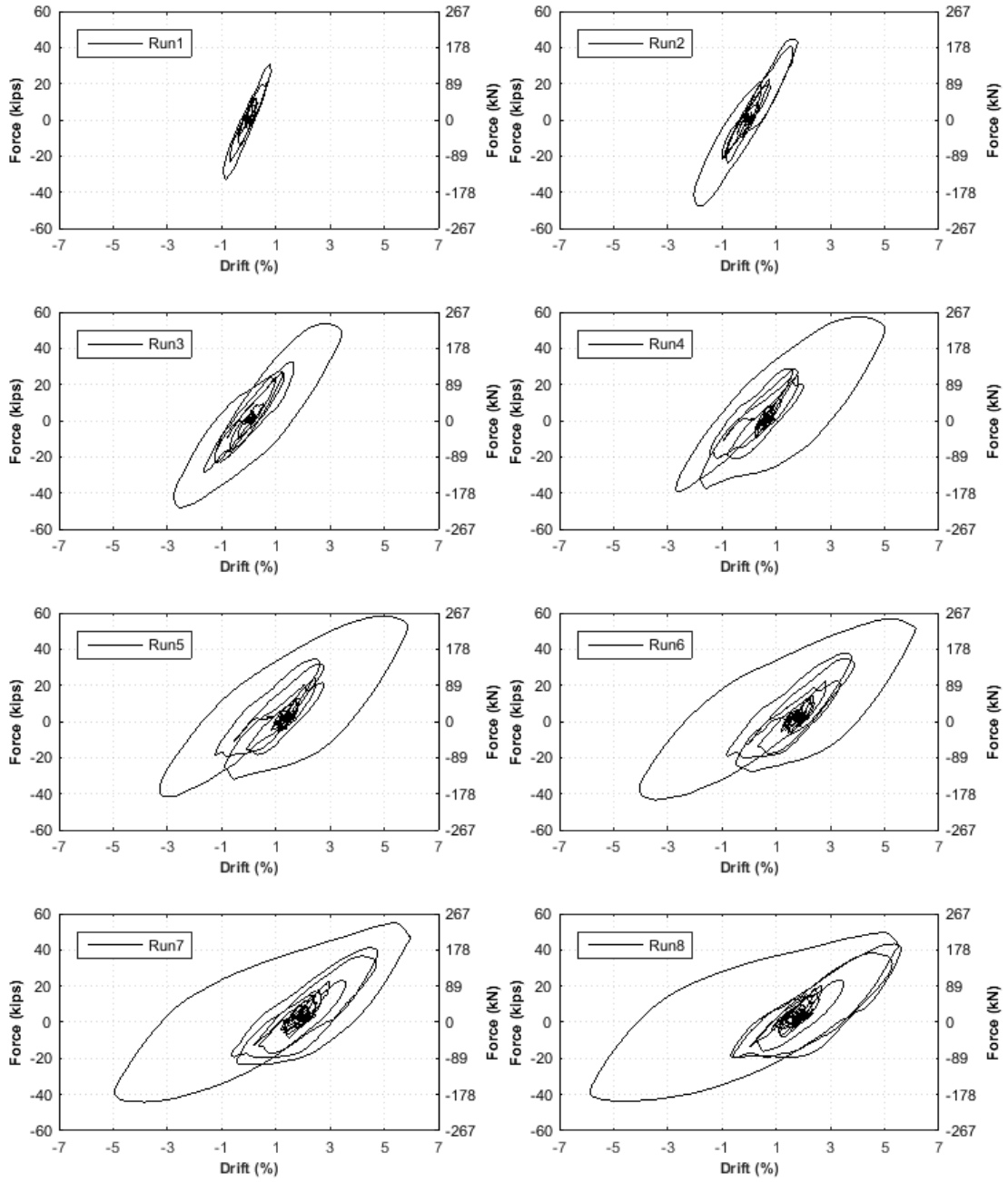

Fig. 71 – Measured force-displacement hysteresis curves at each run - Longitudinal direction

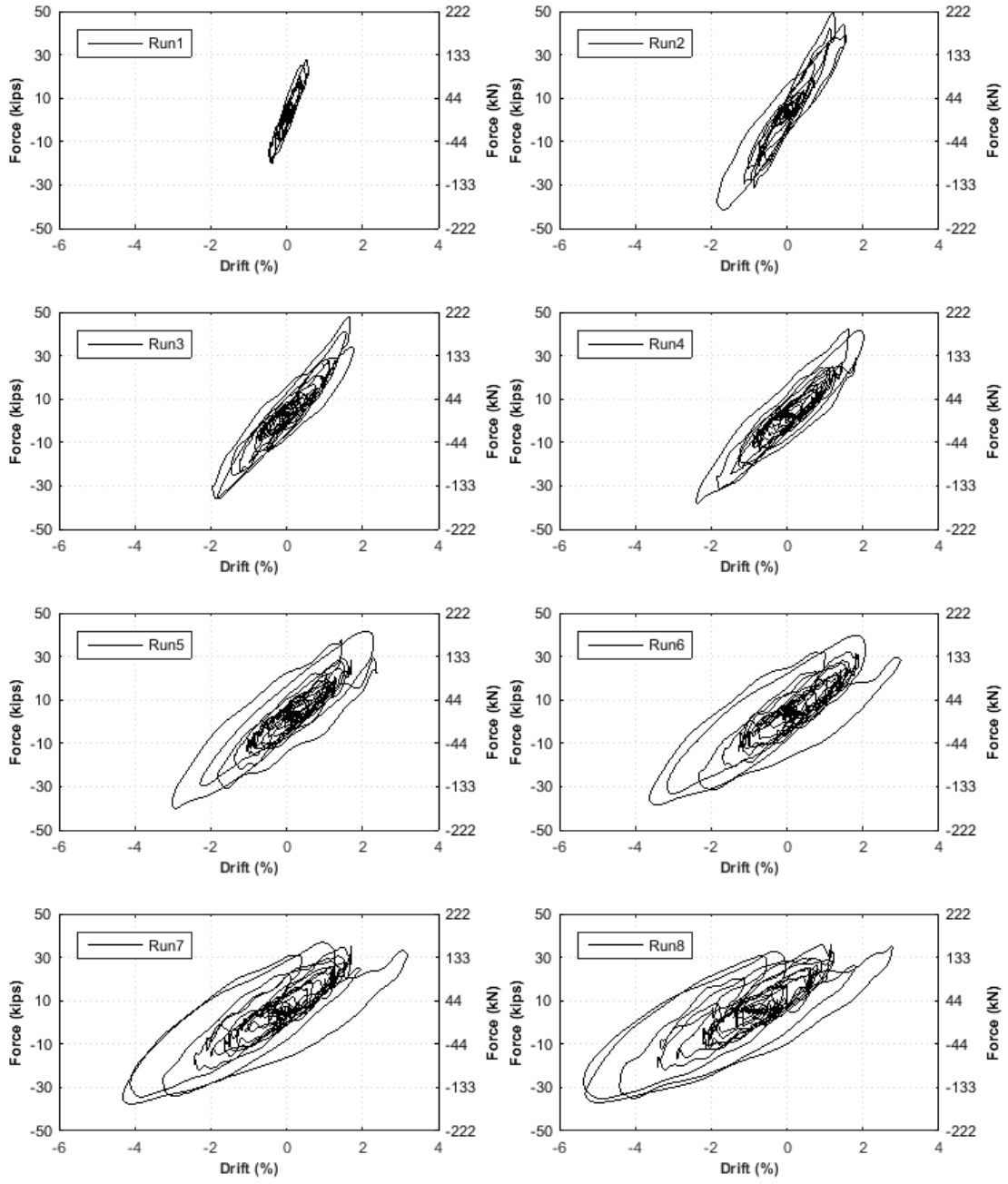

Fig. 72 – Measured force-displacement hysteresis curves at each run – Transverse direction

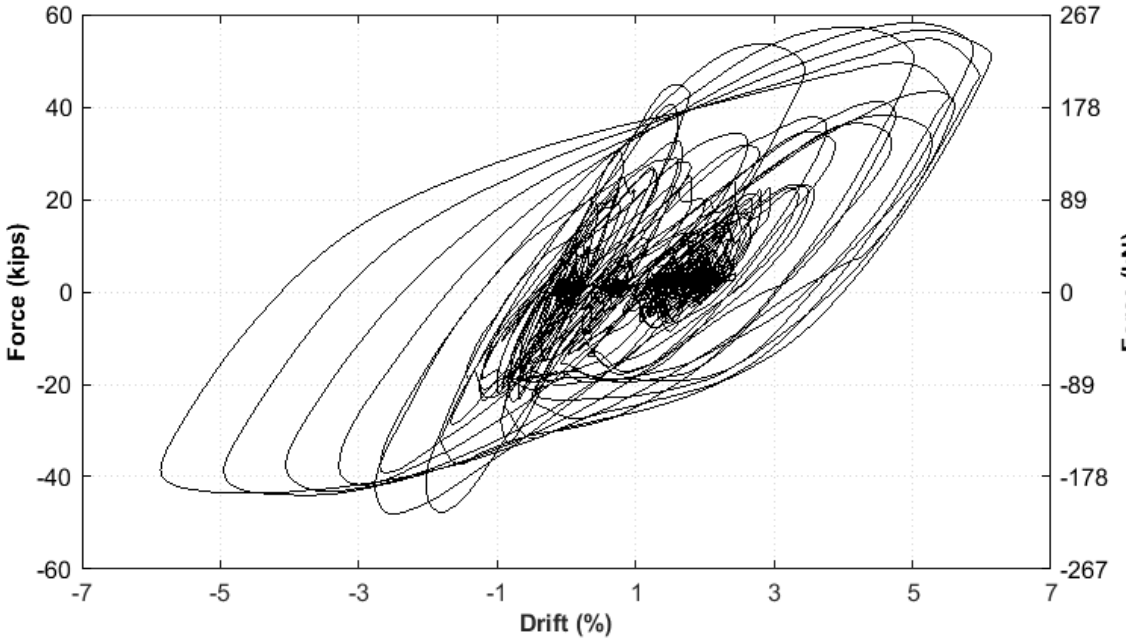

Fig. 73 – Bent cumulative force-displacement relationship – Longitudinal direction

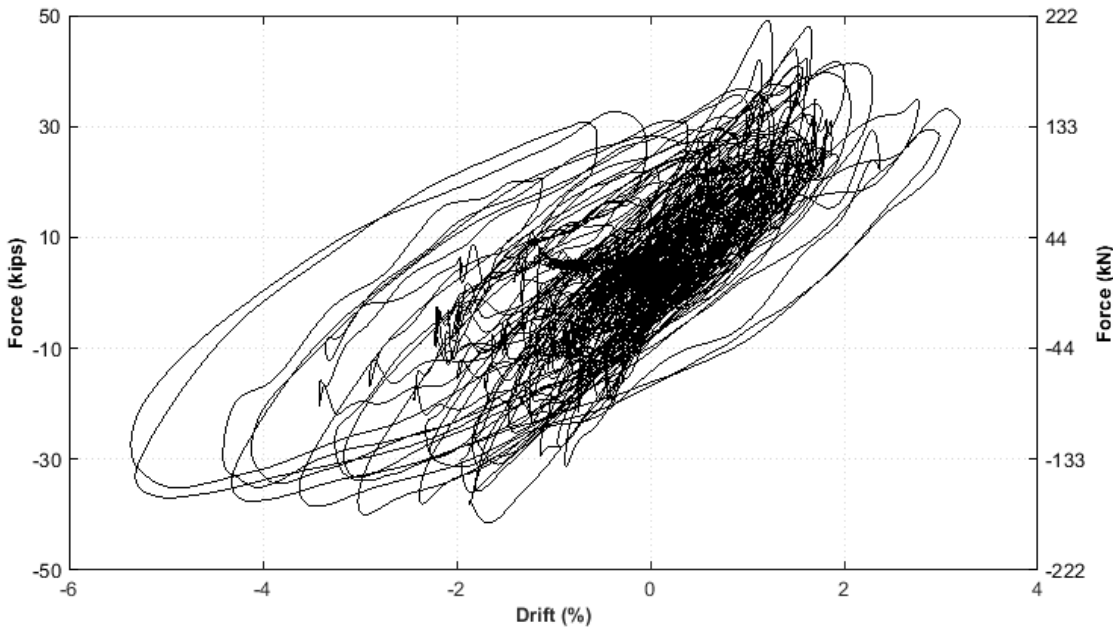

Fig. 74 – Bent cumulative force-displacement relationship – Transverse direction

The apparent displacement ductility of the bent in the longitudinal and transverse direction of the bridge was determined based on the envelopes of the hysteresis curves after idealizing them by an elasto-plastic curve. Fig. 75 shows the envelopes in the positive and negative longitudinal displacement directions, the average of the two, and idealized curve representing the average envelope. Fig. 76 shows the data for the transverse direction.

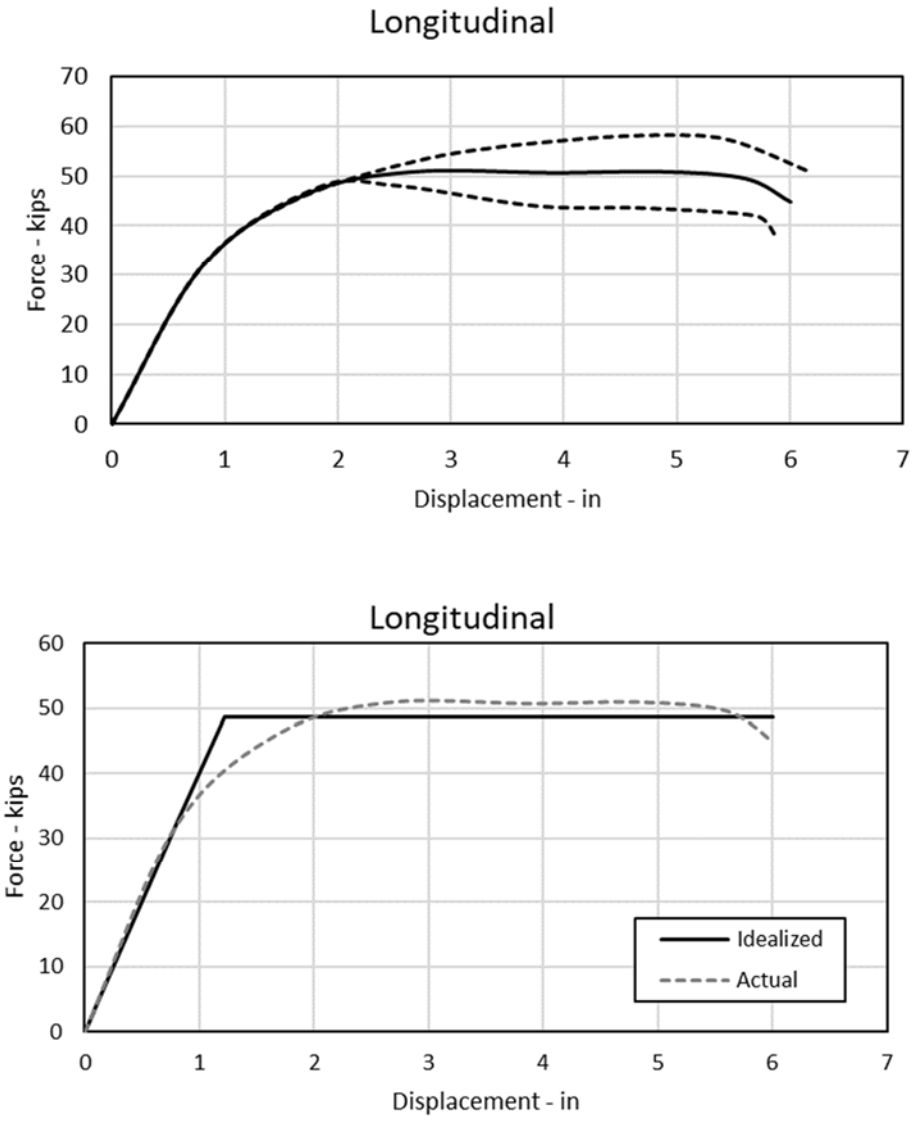

Effective yield disp. =	1.06 in	Effective stiffness =	40 kip/in	**Base shear =**	**48.6 kip**
Ultimate disp. =	5.30 in	Mass =	0.39 kip-s/in^2		
Ductility =	**4.99**	**Period =**	**0.62 sec**		

Fig. 75 – The envelopes, average envelope, and idealized curve in longitudinal direction

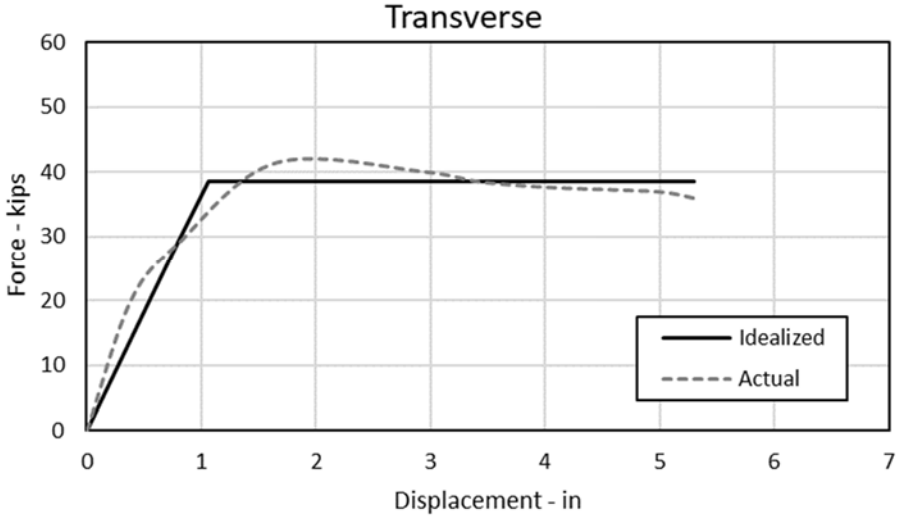

Effective yield disp. =	1.22 in	Effective stiffness =	36.3 kip/in	**Base shear =**	**38.5 kip**
Ultimate disp. =	6.00 in	Mass =	0.39 kip-s/in^2		
Ductility =	**4.94**	**Period =**	**0.65 sec**		

Fig. 76 – The average envelope and idealized curve in transverse direction

It can be seen that the maximum displacement ductility was approximately 5 in each direction corresponding to a resultant displacement ductility capacity of approximately 7, which is comparable to the capacities of CIP bent structures.

A representative sample of the maximum longitudinal bar strain data in the top and bottom of the columns is shown in Fig. 77 and 78, respectively. The measured yield strain was approximately 2400 microstrains. Distance zero in Fig. 77 indicates cap beam column interface. It is clear that the strains peaked at this interface. It is also clear that yielding began mostly in run 2 in the column. The strain at 7 in into the cap beam exceeded the yield strain in successive runs but remained relatively low. The distance zero in Fig. 78 marks the column-footing interface. Substantial yielding took place at this interface, but spread of yielding into the footing and the hinge was limited.

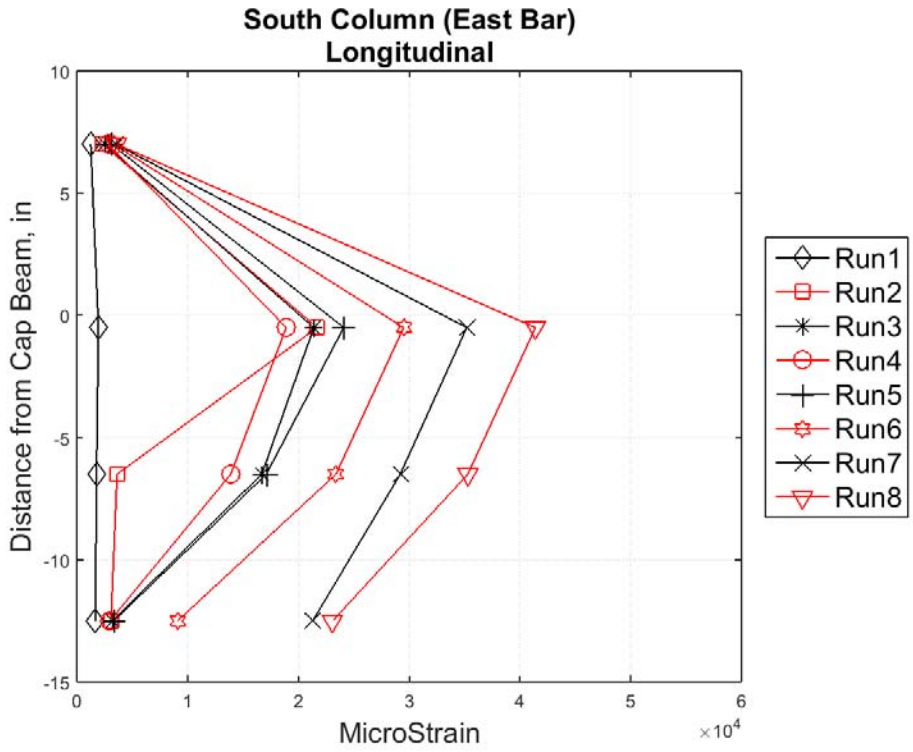

Fig. 77 – Sample column longitudinal bar strain profile in top plastic hinge

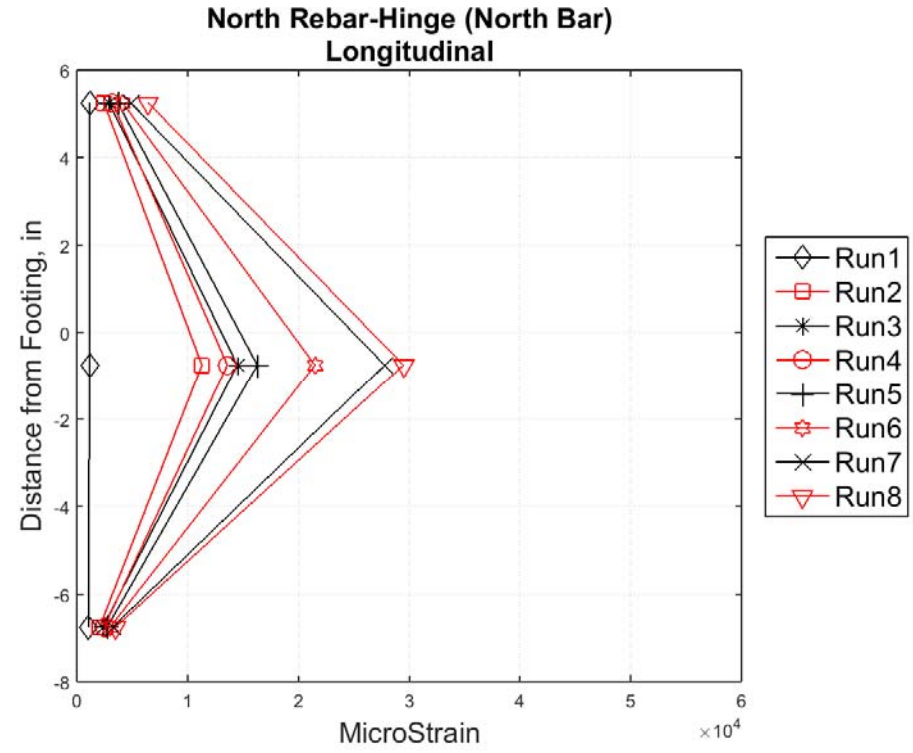

Fig. 78 – Sample column longitudinal bar strain profile in base hinge

The peak strains in the cap beam longitudinal bars were evaluated and were all below the yield strain indicating that the cap beam behaved as a "capacity protected" element and met the design objective. Fig. 79 shows the peak strains for different runs in the bar with the highest strains. This gage was placed on the bottom bar near the column face. The peak strain was less than two-thirds of the yield strain.

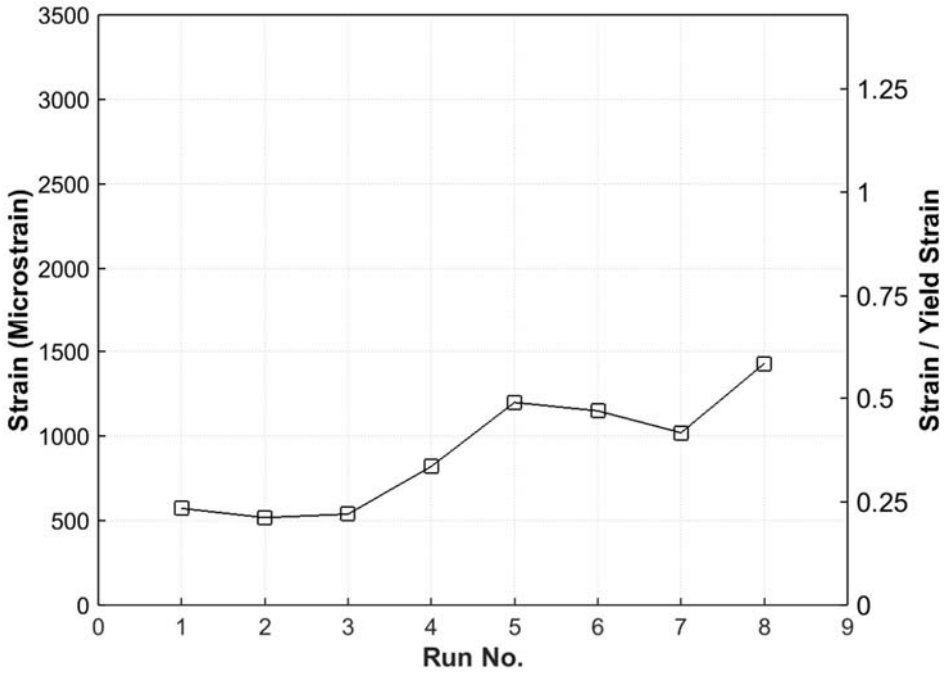

Fig. 79 – Maximum strain in cap beam longitudinal bars at each run

Task 6 – Conduct analytical studies of the bridge model (20% Complete)

Preliminary analytical studies of the bridge model were conducted using the measured material properties and the actual (rather than the target) ground motions. The combined records, excluding the white noise motions that were applied in between the earthquake runs, are shown in Fig. 80. Preliminary analytical results are being obtained and evaluated.

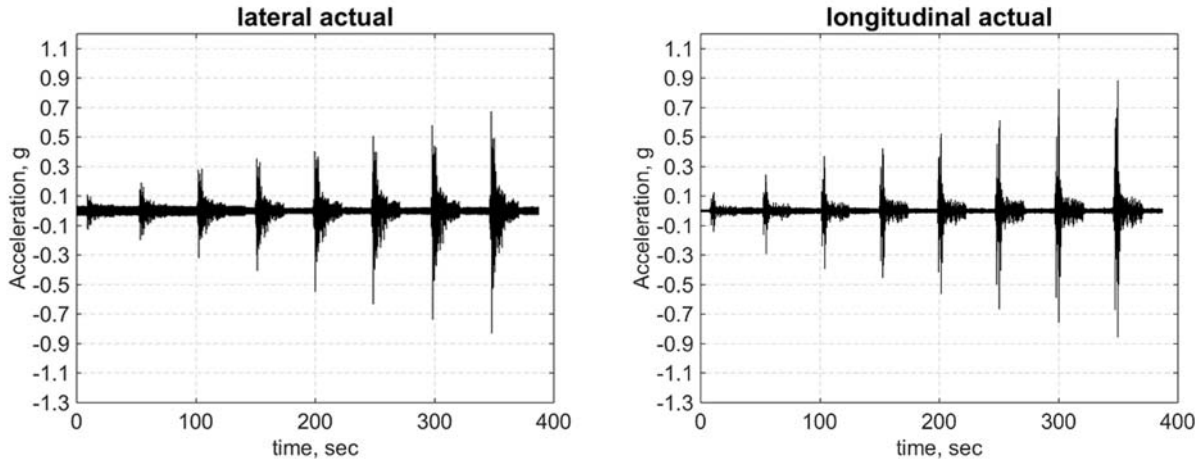

Fig. 80 – Actual acceleration histories recorded in shake table 2 for all the 8 earthquake runs.

Task 7 – Summarize the investigation and the results in final report Pending

A.5 Expected Results and Specific Deliverables

The deliverables from different tasks are as follows:

Task 1: A synthesis of the literature review providing a summary of the state-of-the-art on seismic performance of different prefabricated bridge components and connections.

Task 2: A summary of optimum ABC connections and prefabricated elements with a ranking system.

Task 3: Preliminary plans and dimensions of a 2-span bridge model with connection details at all the joints in addition to the rationale for selection of the prefabricated elements and connections.

Task 4: Finalized plans and details for a 2-span bridge models in addition to instrumentation plans and the earthquake simulation protocol.

Task 5: Key processed data and interpretation of data that are indicative of the bridge seismic performance at the system and component levels in addition to video clips of bridge and connection movements and photos of damage progression at different locations of the bridge models.

Task 6: A reliable analytical modeling method for inelastic seismic analysis of ABC bridge systems.

Task 7: A report summarizing the key steps and procedures used in the study in addition to the data on seismic performance of the bridge model and the related analytical study results. Conclusions regarding component versus system performance of different components, interaction among different components, and variation of load path under different limit states.